

1 A Global Carbon Assimilation System using a modified
2 Ensemble Kalman filter

3
4 Shupeng Zhang^{a,b}, Xiaogu Zheng^{a,b*}, Jing M. Chen^{b,c,d}, Zhuoqi Chen^{a,b}, Bo Dan^{a,b},
5 Xue Yi^{a,b}, Liqun Wang^e and Guocan Wu^{a,b}

6
7
8 *^aCollege of Global Change and Earth System Science,
9 Beijing Normal University, Beijing, China*

10 *^bJoint Center for Global Change Studies, Beijing, China*

11 *^cDepartment of Geography, University of Toronto, Toronto, Canada*

12 *^dInternational Institute for Earth System Science,
13 Nanjing University, Nanjing, China*

14 *^eDepartment of Statistics, University of Manitoba, Winnipeg, Canada*

15
16
17 *Correspondence to: X. Zheng, College of Global Change and Earth System Science,
18 Beijing Normal University, #19 Xijiekouwai St, Beijing, 100875 China, Email:
19 x.zheng@bnu.edu.cn
20

1

2 **Abstract**

3

4 A Global Carbon Assimilation System based on the Ensemble Kalman filter
5 (GCAS-EK) is developed for assimilating atmospheric CO₂ data into an ecosystem
6 model to simultaneously estimate the surface carbon fluxes and atmospheric CO₂
7 distribution. This assimilation approach is similar to CarbonTracker, but with several
8 new developments, including inclusion of atmospheric CO₂ concentration in state
9 vectors, using the Ensemble Kalman filter (EnKF) with one-week assimilation
10 windows, using analysis states to iteratively estimate ensemble forecast errors, and a
11 maximum likelihood estimation of the inflation factors of the forecast and observation
12 errors. The proposed assimilation approach is used to estimate the terrestrial
13 ecosystem carbon fluxes and atmospheric CO₂ distributions from 2002 to 2008. The
14 results show that this assimilation approach can effectively reduce the biases and
15 uncertainties of the carbon fluxes simulated by the ecosystem model.

16

17 **Keywords:** Data assimilation, Ensemble Kalman filter, Ecosystem modeling,
18 Atmospheric transport, CO₂ mole fraction, Surface carbon fluxes

19

1

2 **1 Introduction**

3

4 The carbon dioxide concentration in the atmosphere plays an essential role in the
5 study of global change for its potential to warm up the atmosphere and the surface. A
6 better estimation of carbon fluxes over global ecosystems would help better
7 understand each nation's contribution to global warming and improve the global
8 warming science.

9 In the past decade, many efforts have been made to estimate the surface CO₂
10 fluxes using both atmosphere-based top-down and land-based bottom-up methods.
11 CarbonTracker (Peters et al., 2005; Peters et al., 2007) may be one of the most
12 advanced among these efforts. It uses an ensemble square root filter to assimilate
13 atmospheric CO₂ mole fractions into an ecosystem model coupled with an
14 atmospheric transport model.

15 The model state vectors in CarbonTracker are carbon fluxes only. However, the
16 observed CO₂ consists of both initial state of atmosphere CO₂ and recently released
17 carbon fluxes, so including CO₂ concentration in the state vectors should improve the
18 estimation of initial atmosphere CO₂ (Miyazaki et al., 2011). This could lead to
19 further improvement of carbon flux estimation. Kang et al. (2011) and Liu et al. (2012)
20 also added CO₂ concentrations to the state vectors due to their strong correlations with
21 weather variables that are simultaneously assimilated. However, their efforts mainly
22 focus on studying the performance of the assimilation methodology and observation
23 settings by using idealized models only, not on assimilating real observations.

24 The length of the assimilation window in CarbonTracker is 5 weeks. This would
25 include CO₂ observations far from the analysis time. However this may not

1 necessarily improve the flux analysis compared to an instantaneous analysis due to the
2 attenuation of the detailed information as discussed by Enting (2002). A shorter
3 assimilation window reduces the attenuation of observed CO₂ information, because
4 the analysis system can use near-surface CO₂ observations before the transport of CO₂
5 blurs out the essential information of near-surface CO₂ forcing (Kang et al., 2012).

6 It is well known that correct estimation of the forecast error statistics is crucial for
7 the accuracy of any data assimilation algorithm. In all existing EnKF assimilations for
8 estimating carbon fluxes, the ensemble forecast errors are estimated by the difference
9 of perturbed forecasts and their ensemble mean. The perturbed forecast errors are
10 defined as the perturbed forecast states minus the true state. Motivated by the fact that
11 the analysis state is a better estimate of the true state than the forecast state, Wu et al.
12 (2013) proposed a new estimator for the perturbed forecast errors by using the
13 difference between the perturbed forecast states and the analysis state. Moreover, they
14 demonstrated through a simulation study that the new estimator can lead to better
15 assimilations for models with large errors. Since the errors of ecosystem models are
16 generally large, the new estimation of the perturbed forecast errors is potentially
17 useful to improve EnKF assimilation for estimating carbon fluxes.

18 Besides forecast errors, the observation errors need also be accurately estimated.
19 In majority of schemes for estimating carbon fluxes, including CarbonTracker, the
20 observation error variances are not estimated but empirically assigned. The quality of
21 the estimation of observation error variances critically depends on whether the
22 forecast error covariance matrix is appropriately estimated (Desroziers et al., 2005).
23 However, appropriate estimation of the forecast error covariance matrix is a challenge
24 in real applications.

25 In this paper, we propose several modifications to the conventional EnKF for

1 assimilating atmospheric CO₂ observations into ecosystem models. Firstly, the model
2 state contains both the surface carbon fluxes and atmospheric CO₂ concentration as
3 suggested by Miyazaki et al. (2011), Kang et al. (2011) and Liu et al. (2012).
4 Secondly, the analysis state is used to adaptively estimate forecast errors as suggested
5 by Wu et al. (2013) and Zheng et al. (2013), and both forecast and observation errors
6 are inflated as suggested by Liang et al. (2012). Finally, the one-week assimilation
7 window is tested against longer windows. This modified EnKF is used to assimilate
8 real CO₂ concentration data into the Boreal Ecosystem Productivity Simulator (BEPS,
9 Chen et al., 1999; Liu et al., 1999; Mo et al., 2008) for estimating the real terrestrial
10 carbon fluxes with 3 hourly and 1°×1° resolution from 2002 to 2008.

11 This paper consists of 6 sections. The models and data used in this study are
12 introduced in Section 2, while the methodology is described in Section 3. Section 4
13 presents the validations of the new methodologies using the real observing system.
14 A real data application of the proposed methodology is presented in Section 5.
15 Conclusions and discussions are given in Sections 6.

16

17 **2 Models and Data**

18

19 *2.1 Surface carbon flux models*

20

21 The surface carbon fluxes mainly arise from fossil fuel combustion, vegetation fire,
22 oceanic exchange and biosphere. In this study, only the surface carbon fluxes from
23 biosphere are simulated using BEPS, while the rests are taken from datasets of
24 CarbonTracker 2011 (<http://www.esrl.noaa.gov/gmd/ccgg/carbontracker/>).

25 BEPS is a process-based ecosystem model mainly developed to simulate forest

1 ecosystem carbon budgets (Chen et al., 1999; Ju et al., 2006; Liu et al., 1999). For
2 many reasons, including the complexity of ecosystem processes, spatial-temporal
3 variabilities, and representative errors, parameters in process-based models often do
4 not represent their true values when these models are used to calculate carbon budgets
5 over large areas or for long time periods (Mo et al., 2008). Errors in these parameters
6 lead to biases in model results (Other uncertainties, such as lack of knowledge on
7 historical land-use change and land management, also have influence on model
8 results). In this study, we try to reduce biases in the BEPS-simulated carbon fluxes by
9 incorporating atmospheric CO₂ concentration measurements with data assimilation
10 methods. The prior carbon fluxes simulated by BEPS are at a spatial resolution of
11 1°×1° and for every one hour. On each model grid, BEPS calculates carbon fluxes of
12 6 different plant function types and outputs the sum of them through weighting the
13 fluxes against areal fractions of the plant function types. Figure 1 shows the plant
14 function types with the largest weight on each grid.

15 The vegetation fire flux is taken from CarbonTracker 2011 dataset, which is
16 modeled using the Carnegie-Ames Stanford Approach (CASA) biosphere model
17 (Potter et al., 1993) based on the Global Fire Emission Database (GFED) (van der
18 Werf et al., 2006).

19 The oceanic CO₂ flux is taken from CarbonTracker 2011 optimized results,
20 whose a priori estimates are based on two different datasets: namely ocean inversion
21 flux result (Jacobson et al., 2007) and pCO₂-Clim prior derived from the climatology
22 of seawater pCO₂ (Takahashi et al., 2009).

23 The fossil fuel combustion estimate is the dataset preprocessed by CarbonTracker
24 2011 from the global total fossil fuel emission of the Carbon Dioxide Information and
25 Analysis Center (CDIAC) (Boden et al., 2011) and the “ODIAC” emission dataset

1 (Oda and Maksyutov, 2011).

2

3 *2.2 Atmospheric transport model*

4

5 The global chemical transport Model for OZone And Related chemical Tracers
6 (MOZART,Emmons et al., 2010) is used as the atmospheric transport model. In this
7 study, MOZART is run at a horizontal resolution of approximately $2.8^{\circ}\times 2.8^{\circ}$ with
8 28 vertical levels. The forcing meteorology is from NCAR reanalysis of the National
9 Centers for Environmental Prediction (NCEP) forecasts (Kalnay et al., 1996;Kistler et
10 al., 2001). Since CO₂ is chemically inert in atmosphere, we turn off all the chemical
11 processes and leave only transport of CO₂ by atmospheric motions. Given the
12 atmospheric CO₂ concentration in the previous week and the surface carbon fluxes in
13 the current week, MOZART is used to forecast gridded atmospheric CO₂
14 concentration within the current week.

15

16 *2.3 Observation*

17

18 The atmospheric CO₂ concentration measurements collected and preprocessed by
19 Observation Package (ObsPack) Data Product (Masarie et al., 2014) are used in this
20 study (Product Version:
21 `obspack_co2_1_CARBONTRACKER_CT2013_2014-05-08`). The selected CO₂
22 measurements on 92 sites include observations of two main types: the measurements
23 of air samples at surface sites and in situ quasi-continuous CO₂ time series from
24 towers. Since some stations have multiple observations within a week, on average
25 there are about 140 observations every week during 2002 and 2008. Six laboratories

1 (NOAA Global Monitoring Division, Commonwealth Scientific and Industrial
2 Research Organization, National Center For Atmospheric Research, Environment
3 Canada, Lawrence Berkeley National Laboratory and Instituto de Pesquisas
4 Energeticas e Nucleares) provided these measurements and information of
5 observation sites used in this study is listed in Table 1. CO₂ concentration
6 measurements reflect the variability of the total surface carbon fluxes (i.e. fossil fuel
7 combustion, vegetation fire, oceanic uptake and biosphere) as well as inter-exchange
8 among CO₂ air mass in the initial atmosphere.

9 The observation error variances are also provided in
10 obspack_co2_1_CARBONTRACKER_CT2013_2014-05-08. They were subjectively
11 chosen and manually tuned to fit into specific atmospheric transport models and
12 observations (Peters et al., 2005; Peters et al., 2007). Since these values depend on
13 the atmospheric transport model used in a carbon data assimilation system, they are
14 just used as prior values for this study and will be adaptively adjusted with the
15 proposed assimilation scheme.

16

17 **3 Methodology**

18

19 Within t th week, let \mathbf{c}_t be a set of gridded atmospheric CO₂ concentrations every 3
20 hours, \mathbf{f}_t be the set of prior carbon fluxes every 3 hours, and $\boldsymbol{\lambda}_t$ be a set of factors
21 defined as constants on areas and within a week for adjusting \mathbf{f}_t . Then, the model
22 state is defined as $\mathbf{x}_t = (\mathbf{c}_t^T, \boldsymbol{\lambda}_t^T)^T$. In this study, only land surface carbon fluxes need
23 to be adjusted. The partition of the adjustment factors (i.e. $\boldsymbol{\lambda}_t$) is based on 11
24 TransCom regions (Gurney et al., 2004) and 19 Olson ecosystem types, as in

1 CarbonTracker. Thus the size of the state vector in this study is $128 \times 64 \times 28 \times 8 \times 7$ (\mathbf{c}_t :
 2 $\text{lon} \times \text{lat} \times \text{lev} \times \text{times/day} \times \text{days}$) plus 145 (λ_t). We refer to this data assimilation scheme
 3 as Global Carbon Assimilation System using Ensemble Kalman filter (GCAS-EK).

5 3.1 EnKF with error inflations

6
 7 Using the notations of Ide et al. (1997), the first EnKF algorithm used in this study
 8 consists of the following three main steps:

9 1) Forecast step

10 The perturbed forecast states are estimated as

$$11 \quad \lambda_{t,i}^f = \frac{2}{3} + \frac{1}{3} \lambda_{t-1,i}^a + \xi_{t,i} \quad (1)$$

$$12 \quad \mathbf{c}_{t,i}^f = G(\mathbf{c}_{t-1,i}^a, \lambda_{t,i}^f) \quad (2)$$

13 where i represents an ensemble member, $\xi_{t,i}$ are vectors sampled from a
 14 distribution with mean zero and a given covariance matrix (taken from prior
 15 covariance structure in CarbonTracker, see the document of CarbonTracker and
 16 (Peters et al., 2005; Peters et al., 2007)), and G is the atmospheric transport operator
 17 which maps \mathbf{c}_{t-1} and the λ_t -adjusted \mathbf{f}_t onto gridded CO_2 concentration. Then the
 18 forecast state is estimated as

$$19 \quad \mathbf{x}_t^f = \frac{1}{m} \sum_{i=1}^m \mathbf{x}_{t,i}^f, \quad (3)$$

20 where m is the ensemble size.

21 2) Error step

22 The ensemble forecast errors and the observation error covariance matrix are
 23 estimated as $\sqrt{\theta_t} \mathbf{X}_t^f$ and $\mu_t \mathbf{R}_t$ respectively, where

$$1 \quad \mathbf{X}_t^f = (\mathbf{x}_{t,1}^f - \mathbf{x}_t^f \quad \mathbf{x}_{t,2}^f - \mathbf{x}_t^f \quad \cdots \quad \mathbf{x}_{t,m}^f - \mathbf{x}_t^f), \quad (4)$$

2 and \mathbf{R}_t is the prescribed observation error covariance matrix. θ_t and μ_t are the
3 inflation factors of the forecast error and the observation error respectively which are
4 estimated by minimizing the objective function (Liang et al., 2012;Zheng, 2009):

$$5 \quad -2L_t(\theta, \mu) = \ln \left\{ \det \left(\frac{\theta}{m-1} \mathcal{H}_t(\mathbf{X}_t^f) \mathcal{H}_t(\mathbf{X}_t^f)^\top + \mu \mathbf{R}_t \right) \right\} \\
6 \quad + (\mathbf{y}_t^o - \mathcal{H}_t(\mathbf{x}_t^f))^\top \left(\frac{\theta}{m-1} \mathcal{H}_t(\mathbf{X}_t^f) (\mathcal{H}_t(\mathbf{X}_t^f))^\top + \mu \mathbf{R}_t \right)^{-1} (\mathbf{y}_t^o - \mathcal{H}_t(\mathbf{x}_t^f)) \quad (5)$$

6 where \mathbf{y}_t^o is the vector of atmospheric CO₂ concentration measurements, \mathcal{H}_t is a
7 linear observation operator, which interpolates gridded CO₂ concentrations at
8 observation times and locations. Michalak et al. (2005) used a similar objective
9 function for estimating the statistical parameters in the atmospheric inverse problems
10 of surface fluxes.

11 3) Analysis step

12 The perturbed analysis states are estimated as

$$13 \quad \mathbf{x}_{t,i}^a = \mathbf{x}_{t,i}^f + \sqrt{\theta_t} \mathbf{X}_t^f \left[(m-1) \mathbf{I} + \mathcal{H}_t(\sqrt{\theta_t} \mathbf{X}_t^f)^\top (\mu_t \mathbf{R}_t)^{-1} \mathcal{H}_t(\sqrt{\theta_t} \mathbf{X}_t^f) \right]^{-1} \\
14 \quad \left(\mathcal{H}_t(\sqrt{\theta_t} \mathbf{X}_t^f) \right)^\top (\mu_t \mathbf{R}_t)^{-1} (\mathbf{y}_t^o - \mathcal{H}_t(\mathbf{x}_{t,i}^f) + \boldsymbol{\varepsilon}_{t,i}) \quad (6)$$

15 where $\boldsymbol{\varepsilon}_{t,i}$ is a normal random variable with mean zero and covariance matrix $\mu_t \mathbf{R}_t$
16 (Burgers et al., 1998). The analysis state \mathbf{x}_t^a is estimated as

$$17 \quad \mathbf{x}_t^a = \frac{1}{m} \sum_{i=1}^m \mathbf{x}_{t,i}^a \quad (7)$$

18 Finally, set $t = t + 1$ and return to step (1) for the assimilation at next time step.

19 The assimilated surface carbon fluxes are from all sources because the observed

1 CO₂ concentrations arise from all sources. Then, the surface carbon fluxes from the
2 biosphere are estimated by the assimilated total carbon fluxes minus carbon fluxes
3 from other sources supplied by the forcing data.

4

5 *3.2 Constructing error statistics using analysis*

6

7 Let \mathbf{x}_t^t be the true state. Then the ensemble forecast error should be defined as

8 $\mathbf{x}_{t,i}^f - \mathbf{x}_t^t$. However, \mathbf{x}_t^t is estimated by \mathbf{x}_t^f in Eq.(4). Since \mathbf{x}_t^a is derived by

9 assimilating observations into the model, it is a better estimate of \mathbf{x}_t^t than \mathbf{x}_t^f ,

10 especially when the model error is large (Wu et al., 2013). Therefore after the analysis

11 step 3) in Section 3.1, it is suggested to return to the error step 2), and substitute \mathbf{x}_t^f

12 in Eq.(4) by \mathbf{x}_t^a . This procedure is repeated until the corresponding objective function

13 (Eq.(5)) converges (Wu et al., 2013;Zheng et al., 2013). In this study, the iteration is

14 stopped when the difference between the minima of $-2L_t(\theta, \mu)$ at n -th and $n+1$ th

15 iterations is less one 1. A flowchart of the proposed assimilation scheme is shown in

16 Fig. 2.

17

18 *3.3 Removing carbon mass imbalance*

19

20 In this study, the background CO₂ concentration field at the beginning of a week is the

21 analysis state at the end of the previous week. It is then updated using the

22 observations within the week, so the estimated CO₂ concentration at the beginning of

23 the week is different from that at the end of the previous week. This results in inexact

24 carbon mass balance. To remove this imbalance, a corrected atmospheric CO₂

1 concentration is generated using the sequential forecast of CO₂ concentration with the
 2 optimized carbon fluxes from the very beginning of the entire assimilation period. The
 3 corrected CO₂ concentration is denoted by \mathbf{c}_t^{ca} .

4

5 3.4 Validation statistics

6

7 Chi-square statistics (Tarantola, 2005) are used to test the error covariances
 8 constructed in this study. For the t th week, it is defined as

$$9 \quad \chi_{2,Iter}^2 = (\mathbf{y}_t^o - \mathcal{H}_t(\mathbf{x}_t^f))^T \left(\frac{\theta}{m-1} \mathcal{H}_t(\tilde{\mathbf{X}}_t^f) \mathcal{H}_t(\tilde{\mathbf{X}}_t^f)^T + \mu \mathbf{R}_t \right)^{-1} (\mathbf{y}_t^o - \mathcal{H}_t(\mathbf{x}_t^f)) \quad (8)$$

10 where

$$11 \quad \tilde{\mathbf{X}}_t^f = (\mathbf{x}_{t,1}^f - \mathbf{x}_t^a \quad \mathbf{x}_{t,2}^f - \mathbf{x}_t^a \quad \dots \quad \mathbf{x}_{t,m}^f - \mathbf{x}_t^a) \quad (9)$$

12 and θ , μ are the estimated inflation factors for the week. If the forecast and
 13 observation error covariance matrix are correctly estimated, $\chi_{2,Iter}^2$ follows a
 14 Chi-square distribution with n_{obs} degrees of freedom, where n_{obs} is the number of
 15 observations within t th week. Since the mean and the variance of $\chi_{2,Iter}^2/n_{obs}$ are 1
 16 and $2/n_{obs}$ respectively, the value of $\chi_{2,Iter}^2/n_{obs}$ should be close to 1.

17 The Chi-square statistics for the error covariance matrices without using the
 18 analysis state can be defined similarly to Eq. (8), but with $\tilde{\mathbf{X}}_t^f$ replaced by \mathbf{X}_t^f .
 19 They are denoted as χ_0^2 , χ_1^2 and χ_2^2 for the cases of no inflation, inflation on
 20 forecast error only and inflation on both forecast and observation errors, respectively.
 21 The closer χ_j^2/n_{obs} , $j=0,1,2$ to 1 is, the better the corresponding error statistics.

22 The root mean square error (RMSE) of estimated CO₂ observations is defined as

$$\sqrt{\frac{1}{L} \sum_{i,l} (y_i^{ca}(l) - y_i^o(l))^2} \quad (10)$$

where $y_i^{ca}(l)$ is generated by interpolating c_i^{ca} to the observation site l and time i , and L is the total number of the CO₂ concentration observations during the entire assimilation period. The smaller RMSE means better assimilation scheme.

5

6 **4 Discussions on methodology**

7

8 *4.1 Error covariance statistics*

9

10 To validate the construction of error statistics used in this study, we plot the weekly
 11 time series of $\chi_{2,Iter}^2/n_{obs}$ (Eq. 8) from 2002 to 2003 in Fig. 3, which shows that the
 12 values are remarkably close to 1. In contrast, the weekly time series of χ_0^2/n_{obs} ,
 13 χ_1^2/n_{obs} and χ_2^2/n_{obs} (for the cases of no inflation, inflation on forecast error only
 14 and inflation on both forecast and observation errors) are not as close to 1 as
 15 $\chi_{2,Iter}^2/n_{obs}$. This indicates that the construction of error statistics using the analysis
 16 state iteratively (Section 3.2) is effective for correctly estimating the error statistics.

17 Fig. 3 also shows that χ_2^2/n_{obs} is closer to 1 than χ_1^2/n_{obs} is, and both are
 18 closer to 1 than χ_0^2/n_{obs} is. This suggests that the inflations on forecast error and
 19 observation error are also both effective in improving the estimation of error statistics.

20

21 *4.2 Inclusion of CO₂ concentration in state vectors*

22

23 In this study, the CO₂ concentration is included in state vectors. The benefit of this

1 inclusion needs to be tested against the traditional approach without this inclusion.
2 This issue is studied with the one-week assimilation window.

3 For this purpose we design a comparative experiment as follows. In every week,
4 the CO₂ concentration (i.e. c) is not updated (Eq. 6). Instead the analysis CO₂
5 concentration is derived by sequentially predicting atmospheric CO₂ concentration
6 forced by the updated flux within the week. The carbon mass is automatically
7 balanced in this experiment. The results show that RMSE of the analysis CO₂
8 concentration observations (Eq. 10) is 8.5% larger than that of the corrected analysis
9 CO₂ concentration described in Section 3.3. This suggests that inclusion of CO₂
10 concentration in state vectors can significantly alter the CO₂ mass balance and may
11 have advantage in optimizing the surface CO₂ flux.

12 If the CO₂ concentration is not included in state vectors, the analysis CO₂
13 concentration at the beginning of each week is just the analysis CO₂ concentration at
14 the end of the previous week, so the CO₂ concentration observations within the
15 current week are not used to optimize the CO₂ concentration at the beginning of each
16 week. However, when the CO₂ concentration is included in state vectors, all the
17 observations within the current week and the previous weeks are used to estimate the
18 CO₂ concentration at the beginning of the current week. So the CO₂ concentration at
19 the beginning of each week estimated by inclusion of CO₂ concentration in state
20 vectors could be more accurate than estimated without inclusion. Therefore, the
21 estimated flux associated with the updated CO₂ concentration at the beginning of the
22 current week should have better quality. This is demonstrated by smaller RMSE (Eq.
23 10) with the inclusion than that without the inclusion.

24

25 *4.3 Length of assimilation window*

1

2 Different lengths of the assimilation window are used in various systems (5 weeks in
3 CarbonTracker, 3 and 7 days in Miyazaki et al. (2011) and 6 hours in Kang et al.
4 (2012)). We choose the one-week assimilation window in our methodology for the
5 following reasons. First, since most surface stations only have weekly observations,
6 we need at least one week data to cover the globe. Second, beyond one week the
7 errors of the atmospheric transport model may be significant, and they are very
8 difficult to quantify. Third, the detailed information of observations may be attenuated
9 with time by atmospheric diffusion and advection (Enting, 2002).

10 For comparison to longer assimilation windows, the following alternative
11 experiments with moving assimilation windows were carried out. In the first
12 alternative experiment, the length of the moving window is set to be two weeks while
13 the forecast time step is still one week. The CO₂ concentration observation system is
14 still the same as that described in Section 3, but is used to update the global carbon
15 flux and the atmospheric CO₂ concentration within the current week and the previous
16 week. This procedure is similar to Eq. 6, while the ensemble forecast state of the first
17 week in the assimilation window is set as its ensemble analysis state at previous
18 assimilation time step. Therefore carbon fluxes and CO₂ concentration every week are
19 optimized twice with the observations in the current week and the next week. The
20 corrected analysis of CO₂ concentration is also retrieved from reruning the
21 atmospheric transport model as described in Section 3.3. The second alternative
22 experiment is similar to the first one, but with the three-week moving window.

23 The linear trends for the observations, the estimates with one-week, two-week
24 and three-week moving windows are 2.14ppm yr⁻¹, 2.17 ppm yr⁻¹, 1.59 ppm yr⁻¹, and
25 1.13 ppm yr⁻¹ respectively. It seems that the longer the moving window is, the larger

1 difference is the long term growth rate to the measurements. For further investigating
2 the reason, the annual mean carbon budgets on 11 Transcom regions are shown in Fig.
3 4. It can be found that the longer the moving window is, the larger are the carbon
4 budget adjustments. Long windows result in underestimation of the corresponding
5 long term growth rate.

6 To further investigate the long time and long distance impact of atmospheric
7 transport on CO₂ observations, components of CO₂ concentration at observation sites
8 associated with different Transcom regions in each day before their observation times
9 are calculated in the following way. For a given region and some day before the
10 observation time, prior fluxes on other regions and in other days are all masked. Then
11 the atmospheric transport model can be run with a homogeneous initial atmospheric
12 CO₂ concentration and forced by the masked fluxes to obtain the corresponding CO₂
13 concentration components.

14 These components at individual sites are then averaged in time to investigate
15 general impacts of carbon fluxes from different sources. The results at 7 selected sites
16 are shown in Fig. 5. For these sites, CO₂ concentrations resulting from carbon fluxes
17 within 25 days are mainly from local carbon fluxes within 7 days (although mostly
18 within 3 days). Carbon fluxes beyond 7 days or regions far from the observation
19 locations have very small impacts, indicating that they have little information in
20 observations (i.e. the contribution is less than observation error), even if the
21 atmospheric transport model is accurate. Actually majority of observations
22 (approximately 49) over continental sites used in this study have similar properties to
23 these 7 sites. If the errors of the transport and ecosystem models are considered, the
24 information of fluxes one week before may be even more difficult to estimate.

25 The setting of length of the assimilation window is closely related to spatial and

1 temporal localizations of forecast errors. For the observation network and the
2 atmospheric transport model used in this study, the one-week assimilation window
3 seems most suitable.

4

5 **5 Application and results**

6

7 In this section we use the data assimilation methods described in Section 3 to estimate
8 the land surface carbon fluxes from 2002 to 2008.

9

10 *5.1 Adjustment to total carbon budget of BEPS*

11

12 We first carry out a control run starting from January 1, 2002 with no adjustment of
13 prior fluxes. The simulated CO₂ concentrations are interpolated at observation times
14 and locations, and compared with real observations in the year 2005. The result in Fig.
15 6a) shows that the simulated concentrations have a bias of 2.945 ppm and an RMSE
16 of 4.525 ppm, implying an underestimation of carbon sinks by BEPS. Using
17 GCAS-EK to estimate the ecosystem fluxes, we carry out another control run and
18 comparisons. The bias and RMSE are reduced to 0.967 ppm and 3.675 ppm,
19 respectively (Fig. 6b).

20 It is worthwhile to point out that the underestimation of carbon sinks by BEPS is
21 conditioned on the estimated carbon fluxes released by fossil fuel and fire, even if the
22 ocean fluxes used in our assimilation system are accurate. As described in Section 2,
23 the observed variability of CO₂ concentration is due to the variability of carbon fluxes
24 from all sources, including fossil fuel combustion, vegetation fire, oceanic uptake and
25 biosphere exchange. If non-biospheric carbon sources are underestimated, the carbon

1 sinks from the biosphere simulated by BEPS would also be underestimated.
2 Nevertheless, our adjustment to carbon sinks simulated by BEPS appears reasonable.

3

4 *5.2 Multiyear average of the global carbon flux distribution*

5

6 Figure 7 shows the distribution of the average global carbon budget from 2002 to
7 2008 where the two spatial patterns of carbon fluxes related to BEPS (BEPS and
8 GCAS-EK) are similar, although they are quite different from that of CarbonTracker
9 2011.

10 Carbon budgets are calculated based on the BEPS ecosystem types and the 11
11 Transcom regions (Fig. 8). Similar to the global distribution maps (Fig. 7), GCAS-EK
12 carbon budgets (Fig. 8) have almost the same property in sources or sinks with that
13 simulated by BEPS. However, they are quite different from that of CarbonTracker
14 2011 in many aspects. For example, for the C4 and the shrub in Australia, BEPS
15 simulates carbon sources while CarbonTracker 2011 shows carbon sinks. Moreover in
16 North America, there is a large carbon sink increase of the GCAS-EK over the BEPS
17 simulated. A further diagnostic (not shown here) reveals that, between October and
18 April, the carbon sinks estimated by CarbonTracker 2011 are much larger than that
19 estimated by GCAS-EK. But between May and September, the carbon sinks estimated
20 by CarbonTracker 2011 and GCAS-EK are very close.

21

22 *5.3 Interannual and seasonal variations*

23

24 The interannual variations of the global total carbon budgets are shown in Fig. 9. It
25 shows that CarbonTracker 2011 predicts the largest multiyear average carbon sink

1 (-3.89 PgC yr⁻¹), compared with the smallest one simulated by BEPS (-2.23 PgC yr⁻¹).
2 The assimilated mean carbon sink (-3.87 PgC yr⁻¹) is virtually identical to that
3 estimated by CarbonTracker 2011. The carbon sinks simulated by BEPS and
4 predicted by CarbonTracker 2011 obviously have more interannual oscillation than
5 that assimilated by GCAS-EK.

6 The monthly variations of the multiyear-averaged carbon budgets before and after
7 the assimilation of BEPS results are compared with that by CarbonTracker 2011 in
8 Fig. 10. Clearly, the seasonal variability of the carbon budgets by CarbonTracker
9 2011 is the largest. The assimilated fluxes based on BEPS have larger sinks in the
10 summer and smaller sources in the winter than those before the assimilation.

11

12 *5.4 Comparison to other flux estimations*

13

14 Two independent gridded carbon flux estimates are compared with GCAS-EK
15 estimates.

16 The first independent dataset is net carbon exchange of U.S. terrestrial
17 ecosystems by Xiao et al. (2011) which is generated by integrating eddy covariance
18 flux measurements and satellite observations from Moderate Resolution Imaging
19 Spectroradiometer (MODIS). The original dataset is during 2002 to 2006 with spatial
20 resolution of 1km and temporal resolution of 8 day. For comparison, Xiao's data were
21 grouped from 1km to 1° spatial resolution. The carbon flux distributions of the
22 multiyear average from 2002 to 2006 over United States are shown in Fig. 11 for
23 Xiao's data, GCAS-EK and CarbonTracker 2011. It shows that spatial pattern of the
24 flux assimilated by GCAS-EK is closer to Xiao's data (with spatial standard deviation
25 153 gC m² yr⁻¹ and spatial correlation 0.47) than that by CarbonTracker 2011 (with

1 spatial standard deviation $197 \text{ gC m}^2 \text{ yr}^{-1}$ and spatial correlation 0.22).

2 The carbon budgets estimated by GCAS-EK were also compared to those by
3 Lauvaux et al. (2012), Penn State University (PSU) inversion and Colorado State
4 University (CSU) inversion (Schuh et al., 2013) for the Mid Continent Intensive (MCI)
5 area from June – December 2007. The spatial patterns by GCAS-EK and
6 CarbonTracker 2011 are similar to those estimated by PSU, CSU (Schuh et al., 2013)
7 and Lauvaux et al. (2012) (not shown here). The regional averaged carbon sinks
8 estimated by GCAS-EK and by CarbonTracker 2011 are 0.19 PgC and 0.26 PgC
9 respectively while the averaged carbon sinks estimated by PSU and CSU (Schuh et al.,
10 2013) and by Lauvaux et al. (2012) are between 0.14 PgC and 0.18 PgC, which are
11 closer to that estimated by GCAS-EK than that by CarbonTracker 2011.

12 Since the true values of carbon flux are unknown, the closeness to the
13 independent gridded carbon flux estimates does not mean a better assimilation.
14 However, these two examples indicate that the carbon fluxes estimated by GCAS-EK
15 may provide some useful new information of global carbon flux estimation to the
16 atmospheric inversion community. Therefore, the development of the new
17 assimilation system is worthwhile.

18

19 **6 Conclusion**

20

21 We propose a methodology to assimilate atmospheric CO_2 concentration into surface
22 carbon fluxes simulated by an ecosystem model. In our framework, CO_2 concentration
23 is included in the state vector, and the assimilation window is restricted to one week.
24 Both forecast and observation errors are inflated, and forecast error statistics are
25 estimated in an adaptive procedure using the analysis states. Generally speaking, these

1 adaptive estimations improve the accuracy of assimilated error statistics in EnKF,
2 which leads to further improvement in the accuracy of analysis states. Importantly,
3 pre-assigned values of the observation error variance are improved if these adaptive
4 procedures are applied.

5 The application of the methodology to real data shows that the assimilated total
6 carbon budgets by GCAS-EK are comparable to those reported by CarbonTracker
7 2011. However, there are significant regional differences between carbon flux
8 distributions assimilated by GCAS-EK and CarbonTracker 2011, which may be
9 attributed to the differences between the ecosystem models, atmospheric transport
10 models or the assimilation methodologies.

11 In our future study, we will investigate the sensitivity of assimilation results to
12 the accuracy of ecosystem and transport models. Also, more observation datasets,
13 such as remote sensing CO₂ column data, will be introduced into the GCAS-EK.

14
15
16

17 ***Acknowledgements*** This work was supported by National Program on Key Basic
18 Research Project of China (Grant No. 2010CB950703), R&D Special Fund for
19 Nonprofit Industry (Meteorology, Grant No. GYHY201206008), Key Technologies
20 Research and Development Program of China (Grant No. 2013BAC05B04) and the
21 Natural Sciences and Engineering Research Council of Canada (NSERC). We would
22 like to thank Prof Peter Rayner and an anonymous reviewer for their valuable
23 comments which lead to much improvement of this paper. We acknowledge all
24 atmospheric data providers to
25 obspack_co2_1_CARBONTRACKER_CT2013_2014-05-08, and those who

1 contributed their data to WDCGG. We grateful acknowledge CarbonTracker 2011
2 results provided by NOAA ESRL, Boulder, Colorado, USA, on the website
3 <http://carbontracker.noaa.gov>.

4

5 **References**

6 Boden, T. A., Marland, G., and Andres, R. J.: Global, Regional, and National Fossil-Fuel
7 CO₂ Emissions, Carbon Dioxide Information Analysis Center, Oak Ridge National
8 Laboratory, U.S. Department of Energy, Oak Ridge, Tenn., U.S.A.,
9 10.3334/CDIAC/00001_V2011, 2011.

10 Burgers, G., Jan van Leeuwen, P., and Evensen, G.: Analysis Scheme in the Ensemble
11 Kalman Filter, *Mon. Weather Rev.*, 126, 1719-1724,
12 10.1175/1520-0493(1998)126<1719:asitek>2.0.co;2, 1998.

13 Chen, J. M., Liu, J., Cihlar, J., and Goulden, M. L.: Daily canopy photosynthesis model
14 through temporal and spatial scaling for remote sensing applications, *Ecol. Model.*,
15 124, 99--119, 10.1016/S0304-3800(99)00156-8, 1999.

16 Desroziers, G., Berre, L., Chapnik, B., and Poli, P.: Diagnosis of observation,
17 background and analysis-error statistics in observation space, *Q. J. R. Meteorolog.*
18 *Soc.*, 131, 3385--3396, 2005.

19 Emmons, L. K., Walters, S., Hess, P. G., Lamarque, J. F., Pfister, G. G., Fillmore, D.,
20 Granier, C., Guenther, A., Kinnison, D., Laepple, T., Orlando, J., Tie, X., Tyndall, G.,
21 Wiedinmyer, C., Baughcum, S. L., and Kloster, S.: Description and evaluation of the
22 Model for Ozone and Related chemical Tracers, version 4 (MOZART-4), *Geosci. Model*
23 *Dev.*, 3, 43-67, 10.5194/gmd-3-43-2010, 2010.

24 Enting, I. G.: *Inverse Problems in Atmospheric Constituent Transport*, Cambridge
25 University Press, New York, 2002.

26 Gurney, K. R., Law, R. M., Denning, A. S., Rayner, P. J., Pak, B. C., Baker, D., Bousquet,
27 P., Bruhwiler, L., Chen, Y. H., Ciais, P., Fung, I. Y., Heimann, M., John, J., Maki, T.,
28 Maksyutov, S., Peylin, P., Prather, M., and Taguchi, S.: Transcom 3 inversion
29 intercomparison: Model mean results for the estimation of seasonal carbon sources
30 and sinks, *Global Biogeochem. Cycles*, 18, GB1010-GB1010, 10.1029/2003GB002111,
31 2004.

32 Ide, K., Courtier, P., Ghil, M., and Lorenc, A. C.: Unified notation for data assimilation:
33 Operational, sequential and variational, *J. Meteorol. Soc. Jpn.*, 75, 181-189, 1997.

34 Jacobson, A. R., Mikaloff Fletcher, S. E., Gruber, N., Sarmiento, J. L., and Gloor, M.: A
35 joint atmosphere-ocean inversion for surface fluxes of carbon dioxide: 1. Methods
36 and global-scale fluxes, *Global Biogeochem. Cycles*, 21, GB1019,

- 1 10.1029/2005GB002556, 2007.
- 2 Ju, W. M., Chen, J. M., Black, T. A., Barr, A. G., Liu, J., and Chen, B. Z.: Modelling
3 multi-year coupled carbon and water fluxes in a boreal aspen forest, *Agric. For.*
4 *Meteorol.*, 140, 136--151, 10.1016/j.agrformet.2006.08.008, 2006.
- 5 Kalnay, E., Kanamitsu, M., Kistler, R., Collins, W., Deaven, D., Gandin, L., Iredell, M.,
6 Saha, S., White, G., Woollen, J., Zhu, Y., Leetmaa, A., Reynolds, R., Chelliah, M.,
7 Ebisuzaki, W., Higgins, W., Janowiak, J., Mo, K. C., Ropelewski, C., Wang, J., Jenne, R.,
8 and Joseph, D.: The NCEP/NCAR 40-Year Reanalysis Project, *Bulletin Am. Meteorol.*
9 *Soc.*, 77, 437-471, 10.1175/1520-0477(1996)077<0437:TNYRP>2.0.CO;2, 1996.
- 10 Kang, J. S., Kalnay, E., Liu, J., Fung, I., Miyoshi, T., and Ide, K.: "Variable localization" in
11 an ensemble Kalman filter: Application to the carbon cycle data assimilation, *J.*
12 *Geophys. Res.*, 116, D09110, 2011.
- 13 Kang, J. S., Kalnay, E., Miyoshi, T., Liu, J., and Fung, I.: Estimation of surface carbon
14 fluxes with an advanced data assimilation methodology, *J. Geophys. Res.: Atmos.*
15 (1984--2012), 117, 2012.
- 16 Kistler, R., Collins, W., Saha, S., White, G., Woollen, J., Kalnay, E., Chelliah, M.,
17 Ebisuzaki, W., Kanamitsu, M., Kousky, V., van den Dool, H., Jenne, R., and Fiorino, M.:
18 The NCEP-NCAR 50-Year Reanalysis: Monthly Means CD-ROM and Documentation,
19 *Bulletin Am. Meteorol. Soc.*, 82, 247-267,
20 10.1175/1520-0477(2001)082<0247:TNNYRM>2.3.CO;2, 2001.
- 21 Lauvaux, T., Schuh, A. E., Uliasz, M., Richardson, S., Miles, N., Andrews, A. E., Sweeney,
22 C., Diaz, L. I., Martins, D., Shepson, P. B., and Davis, K. J.: Constraining the CO₂ budget
23 of the corn belt: exploring uncertainties from the assumptions in a mesoscale inverse
24 system, *Atmos. Chem. Phys.*, 12, 337-354, 10.5194/acp-12-337-2012, 2012.
- 25 Liang, X., Zheng, X., Zhang, S., Wu, G., Dai, Y., and Li, Y.: Maximum likelihood
26 estimation of inflation factors on error covariance matrices for ensemble Kalman
27 filter assimilation, *Q. J. R. Meteorol. Soc.*, 138, 263--273, 10.1002/qj.912, 2012.
- 28 Liu, J., Chen, J. M., Cihlar, J., and Chen, W.: Net primary productivity distribution in
29 the BOREAS region from a process model using satellite and surface data, *J. Geophys.*
30 *Res. [Atmos.]*, 104, 27735--27754, 10.1029/1999JD900768, 1999.
- 31 Liu, J., Fung, I., Kalnay, E., Kang, J.-S., Olsen, E. T., and Chen, L.: Simultaneous
32 assimilation of AIRS Xco₂ and meteorological observations in a carbon climate model
33 with an ensemble Kalman filter, *J. Geophys. Res. [Atmos.]*, 117, D05309,
34 10.1029/2011JD016642, 2012.
- 35 Masarie, K. A., Peters, W., Jacobson, A. R., and Tans, P. P.: ObsPack: a framework for
36 the preparation, delivery, and attribution of atmospheric greenhouse gas
37 measurements, *Earth Syst. Sci. Data*, 6, 375-384, 10.5194/essd-6-375-2014, 2014.
- 38 Michalak, A. M., Hirsch, A., Bruhwiler, L., Gurney, K. R., Peters, W., and Tans, P. P.:

- 1 Maximum likelihood estimation of covariance parameters for Bayesian atmospheric
2 trace gas surface flux inversions, *J. Geophys. Res. [Atmos.]*, 110, D24107,
3 10.1029/2005JD005970, 2005.
- 4 Miyazaki, K., Maki, T., Patra, P., and Nakazawa, T.: Assessing the impact of satellite,
5 aircraft, and surface observations on CO₂ flux estimation using an ensemble-based
6 4-D data assimilation system, *J. Geophys. Res. [Atmos.]*, 116, D16306,
7 10.1029/2010JD015366, 2011.
- 8 Mo, X. G., Chen, J. M., Ju, W. M., and Black, T. A.: Optimization of ecosystem model
9 parameters through assimilating eddy covariance flux data with an ensemble Kalman
10 filter, *Ecol. Model.*, 217, 157--173, 10.1016/j.ecolmodel.2008.06.021, 2008.
- 11 Oda, T., and Maksyutov, S.: A very high-resolution (1 km×1 km) global fossil fuel CO₂
12 emission inventory derived using a point source database and satellite observations
13 of nighttime lights, *Atmos. Chem. Phys.*, 11, 543-556, 10.5194/acp-11-543-2011,
14 2011.
- 15 Peters, W., Miller, J. B., Whitaker, J., Denning, A. S., Hirsch, A., Krol, M. C., Zupanski, D.,
16 Bruhwiler, L., and Tans, P. P.: An ensemble data assimilation system to estimate CO₂
17 surface fluxes from atmospheric trace gas observations, *J. Geophys. Res. [Atmos.]*,
18 110, D24304-D24304, 10.1029/2005JD006157, 2005.
- 19 Peters, W., Jacobson, A. R., Sweeney, C., Andrews, A. E., Conway, T. J., Masarie, K.,
20 Miller, J. B., Bruhwiler, L. M., Petron, G., Hirsch, A. I., Worthy, D. E., van der Werf, G. R.,
21 Randerson, J. T., Wennberg, P. O., Krol, M. C., and Tans, P. P.: An atmospheric
22 perspective on North American carbon dioxide exchange: CarbonTracker, *Proceedings*
23 *of the National Academy of Sciences of the United States of America*, 104,
24 18925-18930, 10.1073/pnas.0708986104, 2007.
- 25 Potter, C. S., Randerson, J. T., Field, C. B., Matson, P. A., Vitousek, P. M., Mooney, H. A.,
26 and Klooster, S. A.: Terrestrial ecosystem production: A process model based on
27 global satellite and surface data, *Global Biogeochem. Cycles*, 7, 811-841,
28 10.1029/93GB02725, 1993.
- 29 Schuh, A. E., Lauvaux, T., West, T. O., Denning, A. S., Davis, K. J., Miles, N., Richardson,
30 S., Uliasz, M., Lokupitiya, E., Cooley, D., Andrews, A., and Ogle, S.: Evaluating
31 atmospheric CO₂ inversions at multiple scales over a highly inventoried agricultural
32 landscape, *Global Change Biol.*, 19, 1424-1439, 10.1111/gcb.12141, 2013.
- 33 Takahashi, T., Sutherland, S. C., Wanninkhof, R., Sweeney, C., Feely, R. A., Chipman, D.
34 W., Hales, B., Friederich, G., Chavez, F., Sabine, C., and others: Climatological mean
35 and decadal change in surface ocean pCO₂, and net sea-air CO₂
36 flux over the global oceans, *Deep Sea Res. Part II: Topical Studies in*
37 *Oceanography*, 56, 554--577, 2009.
- 38 Tarantola, A.: *Inverse Problem Theory and Methods for Model Parameter Estimation*,
39 *Other Titles in Applied Mathematics*, Society for Industrial and Applied Mathematics,
40 348 pp., 2005.

1 van der Werf, G. R., Randerson, J. T., Giglio, L., Collatz, G. J., Kasibhatla, P. S., and
2 Arellano Jr, A. F.: Interannual variability in global biomass burning emissions from
3 1997 to 2004, *Atmos. Chem. Phys.*, 6, 3423-3441, 10.5194/acp-6-3423-2006, 2006.

4 Wu, G. C., Zheng, X. G., Wang, L. Q., Zhang, S. P., Liang, X., and Li, Y.: A new structure
5 for error covariance matrices and their adaptive estimation in EnKF assimilation, *Q. J.
6 R. Meteorolog. Soc.*, 139, 795-804, Doi 10.1002/Qj.2000, 2013.

7 Xiao, J., Zhuang, Q., Law, B. E., Baldocchi, D. D., Chen, J., Richardson, A. D., Melillo, J.
8 M., Davis, K. J., Hollinger, D. Y., Wharton, S., Oren, R., Noormets, A., Fischer, M. L.,
9 Verma, S. B., Cook, D. R., Sun, G., McNulty, S., Wofsy, S. C., Bolstad, P. V., Burns, S. P.,
10 Curtis, P. S., Drake, B. G., Falk, M., Foster, D. R., Gu, L., Hadley, J. L., Katul, G. G., Litvak,
11 M., Ma, S., Martin, T. A., Matamala, R., Meyers, T. P., Monson, R. K., Munger, J. W.,
12 Oechel, W. C., Paw, U. K. T., Schmid, H. P., Scott, R. L., Starr, G., Suyker, A. E., and Torn,
13 M. S.: Assessing net ecosystem carbon exchange of U.S. terrestrial ecosystems by
14 integrating eddy covariance flux measurements and satellite observations, *Agric. For.
15 Meteorol.*, 151, 60-69, 10.1016/j.agrformet.2010.09.002, 2011.

16 Zheng, X.: An Adaptive Estimation of Forecast Error Covariance Parameters for
17 Kalman Filtering Data Assimilation, *Adv. Atmos. Sci.*, 26, 154--160,
18 10.1007/s00376-009-0154-5, 2009.

19 Zheng, X., Wu, G., Zhang, S., Liang, X., Dai, Y., and Li, Y.: Using analysis state to
20 construct a forecast error covariance matrix in ensemble Kalman filter assimilation,
21 *Adv. Atmos. Sci.*, 30, 1303-1312, 10.1007/s00376-012-2133-5, 2013.

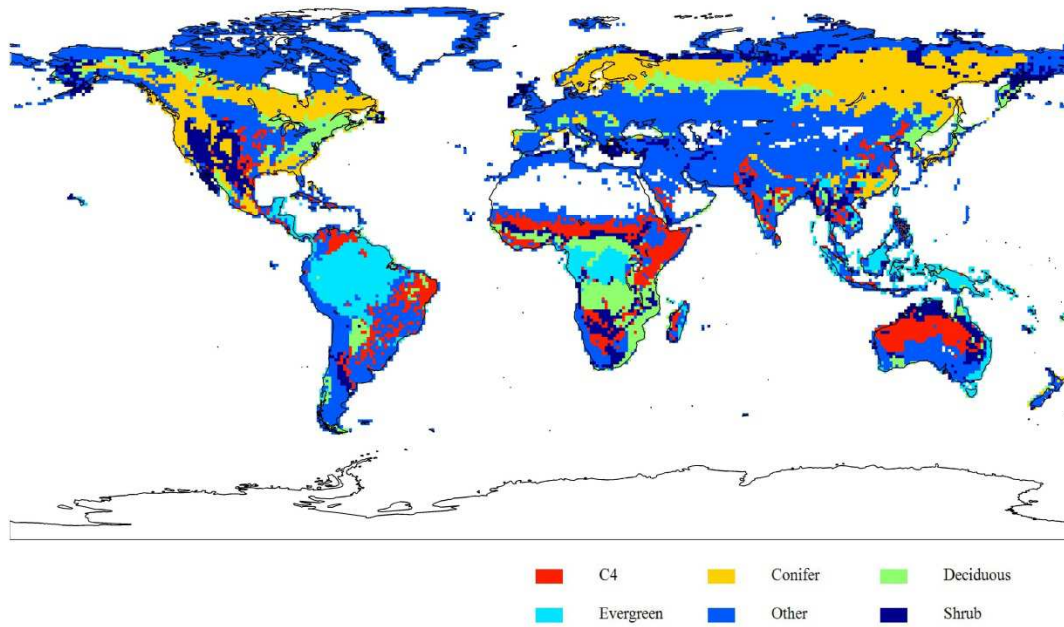
22

1 **Table 1.** 92 observation sites used in this study. "r" refers to prescribed observation
 2 error ($\mu\text{mol } \mu\text{mol}^{-1}$).

Site Code	Lat (°)	Lon (°)	r	Lab	Site Code	Lat (°)	Lon (°)	r	Lab
ABP_01D0	-12.27	-38.17	2.50	NOAA*	MID_01D0	28.21	-177.38	1.50	NOAA
ABP_26D0	-12.27	-38.17	2.50	IPEN*	MKN_01D0	-0.05	37.30	2.50	NOAA
ALT_01D0	82.45	-62.51	1.50	NOAA	MLO_01C0_02LST	19.54	-155.58	0.75	NOAA
ALT_06C0_14LST	82.45	-62.51	2.50	EC*	MLO_01D0	19.54	-155.58	1.50	NOAA
AMT_01C3_14LST	45.03	-68.68	3.00	NOAA	MQA_02D0	-54.48	158.97	0.75	CSIRO
AMT_01P0	45.03	-68.68	3.00	NOAA	NMB_01D0	-23.58	15.03	2.50	NOAA
ASC_01D0	-7.97	-14.40	0.75	NOAA	NWR_01D0	40.05	-105.58	1.50	NOAA
ASK_01D0	23.18	5.42	1.50	NOAA	NWR_03C0_02LST	40.05	-105.58	3.00	NCAR*
AZR_01D0	38.77	-27.38	1.50	NOAA	OBN_01D0	55.11	36.60	7.50	NOAA
BAL_01D0	55.35	17.22	7.50	NOAA	OXK_01D0	50.03	11.80	2.50	NOAA
BAO_01C3_14LST	40.05	-105.00	3.00	NOAA	PAL_01D0	67.97	24.12	2.50	NOAA
BAO_01P0	40.05	-105.00	3.00	NOAA	POC_01D1	-0.39	-132.32	0.75	NOAA
BHD_01D0	-41.41	174.87	1.50	NOAA	PSA_01D0	-64.92	-64.00	0.75	NOAA
BKT_01D0	-0.20	100.32	7.50	NOAA	PTA_01D0	38.95	-123.74	7.50	NOAA
BME_01D0	32.37	-64.65	1.50	NOAA	RPB_01D0	13.17	-59.43	1.50	NOAA
BMW_01D0	32.27	-64.88	1.50	NOAA	SCT_01C3_14LST	33.41	-81.83	3.00	NOAA
BRW_01C0_14LST	71.32	-156.61	2.50	NOAA	SEY_01D0	-4.67	55.17	0.75	NOAA
BRW_01D0	71.32	-156.61	1.50	NOAA	SGP_01D0	36.80	-97.50	2.50	NOAA
BSC_01D0	44.17	28.68	7.50	NOAA	SGP_64C3_16LST	36.80	-97.50	3.00	LBNL*
CBA_01D0	55.21	-162.72	1.50	NOAA	SHM_01D0	52.72	174.10	2.50	NOAA
CDL_06C0_14LST	53.99	-105.12	3.00	EC	SIS_02D0	60.17	-1.17	2.50	CSIRO
CFA_02D0	-19.28	147.06	2.50	CSIRO*	SMO_01C0_14LST	-14.25	-170.56	0.75	NOAA
CGO_01D0	-40.68	144.69	0.75	NOAA	SMO_01D0	-14.25	-170.56	1.50	NOAA
CGO_02D0	-40.68	144.69	0.75	CSIRO	SNP_01C3_02LST	38.62	-78.35	3.00	NOAA
CHR_01D0	1.70	-157.17	0.75	NOAA	SPL_03C0_02LST	40.45	-106.73	3.00	NCAR
CRZ_01D0	-46.45	51.85	0.75	NOAA	SPO_01C0_14LST	-89.98	-24.80	0.75	NOAA
CYA_02D0	-66.28	110.52	0.75	CSIRO	SPO_01D0	-89.98	-24.80	1.50	NOAA
EGB_06C0_14LST	44.23	-79.78	3.00	EC	STM_01D0	66.00	2.00	1.50	NOAA
EIC_01D0	-27.15	-109.45	7.50	NOAA	STR_01P0	37.76	-122.45	3.00	NOAA
ETL_06C0_14LST	54.35	-104.98	3.00	EC	SUM_01D0	72.58	-38.48	1.50	NOAA
FSD_06C0_14LST	49.88	-81.57	3.00	EC	SYO_01D0	-69.00	39.58	0.75	NOAA
GMI_01D0	13.43	144.78	1.50	NOAA	TAP_01D0	36.73	126.13	7.50	NOAA
HBA_01D0	-75.58	-26.50	0.75	NOAA	TDF_01D0	-54.87	-68.48	0.75	NOAA
HPB_01D0	47.80	11.01	7.50	NOAA	THD_01D0	41.05	-124.15	2.50	NOAA
HUN_01D0	46.95	16.65	7.50	NOAA	UTA_01D0	39.90	-113.72	2.50	NOAA
ICE_01D0	63.40	-20.29	1.50	NOAA	UUM_01D0	44.45	111.10	2.50	NOAA
KEY_01D0	25.67	-80.16	2.50	NOAA	WBI_01C3_14LST	41.72	-91.35	3.00	NOAA
KUM_01D0	19.52	-154.82	1.50	NOAA	WBI_01P0	41.72	-91.35	3.00	NOAA
KZD_01D0	44.06	76.82	2.50	NOAA	WGC_01C3_14LST	38.27	-121.49	3.00	NOAA
KZM_01D0	43.25	77.88	2.50	NOAA	WGC_01P0	38.27	-121.49	3.00	NOAA
LEF_01C3_14LST	45.95	-90.27	3.00	NOAA	WIS_01D0	31.13	34.88	2.50	NOAA
LEF_01P0	45.95	-90.27	3.00	NOAA	WKT_01C3_14LST	31.31	-97.33	3.00	NOAA
LLB_06C0_14LST	54.95	-112.45	3.00	EC	WKT_01P0	31.31	-97.33	3.00	NOAA
LMP_01D0	35.52	12.62	1.50	NOAA	WLG_01D0	36.29	100.90	1.50	NOAA
MAA_02D0	-67.62	62.87	0.75	CSIRO	WSA_06C0_14LST	49.93	-60.02	3.00	EC
MHD_01D0	53.33	-9.90	2.50	NOAA	ZEP_01D0	78.90	11.88	1.50	NOAA

3 *"NOAA": NOAA Global Monitoring Division; "CSIRO": Commonwealth Scientific and
 4 Industrial Research Organization; "NCAR": National Center For Atmospheric Research; "EC":
 5 Environment Canada; "IPEN": Instituto de Pesquisas Energeticas e Nucleares; "LBNL":
 6 Lawrence Berkeley National Laboratory.
 7

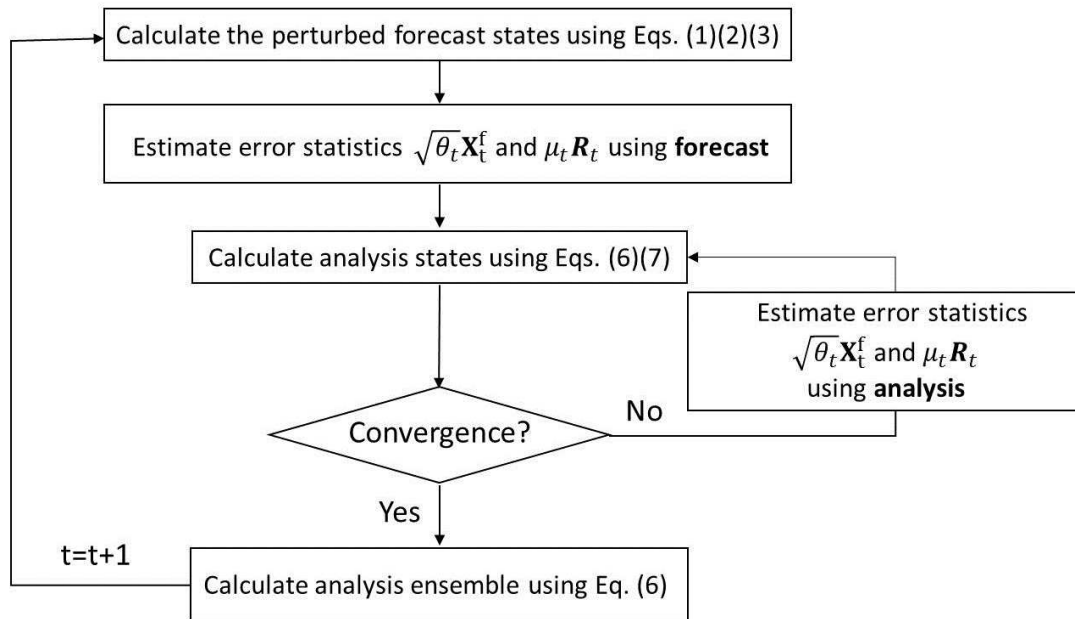
1



2

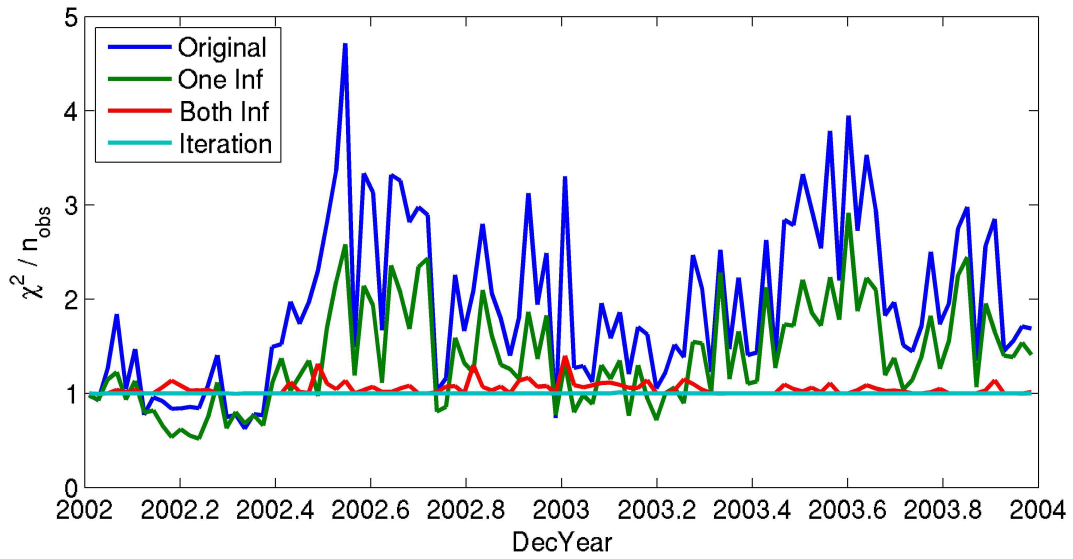
3 **Figure 1.** Land areas of 6 plant function types used in ecosystem model BEPS.

4



1
2
3

Figure 2. Flowchart of modified Ensemble Kalman filter.

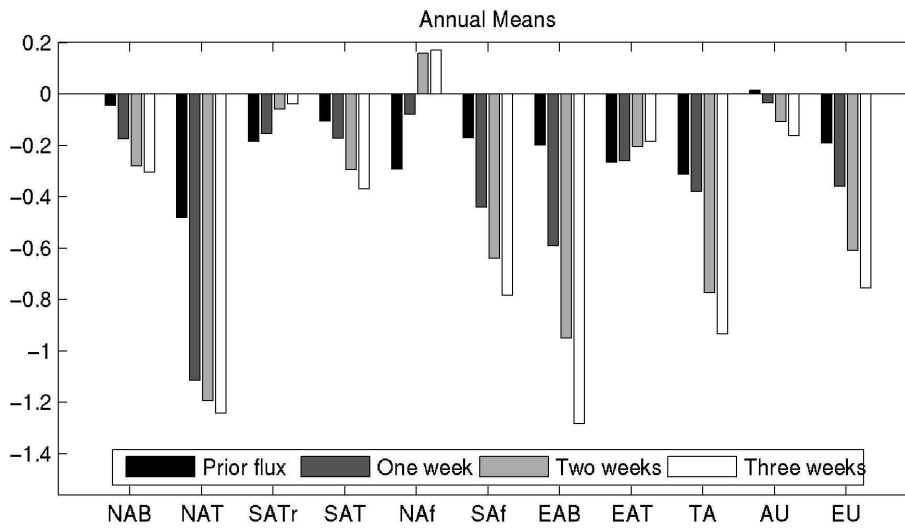


1

2 **Figure 3.** χ^2 statistics of the analysis state for four estimates of error
 3 covariance. “Original” refers to the case without inflations; “One Inf”
 4 refers to the case with inflation on forecast error covariance only; “Both
 5 Inf” refers to the case with inflations on both forecast and observation error
 6 covariances and “Iteration” refers to the case with both inflations and
 7 further using analysis to improve forecast error statistics. The closer
 8 χ^2 / n_{obs} is to 1, the better the corresponding error estimates.

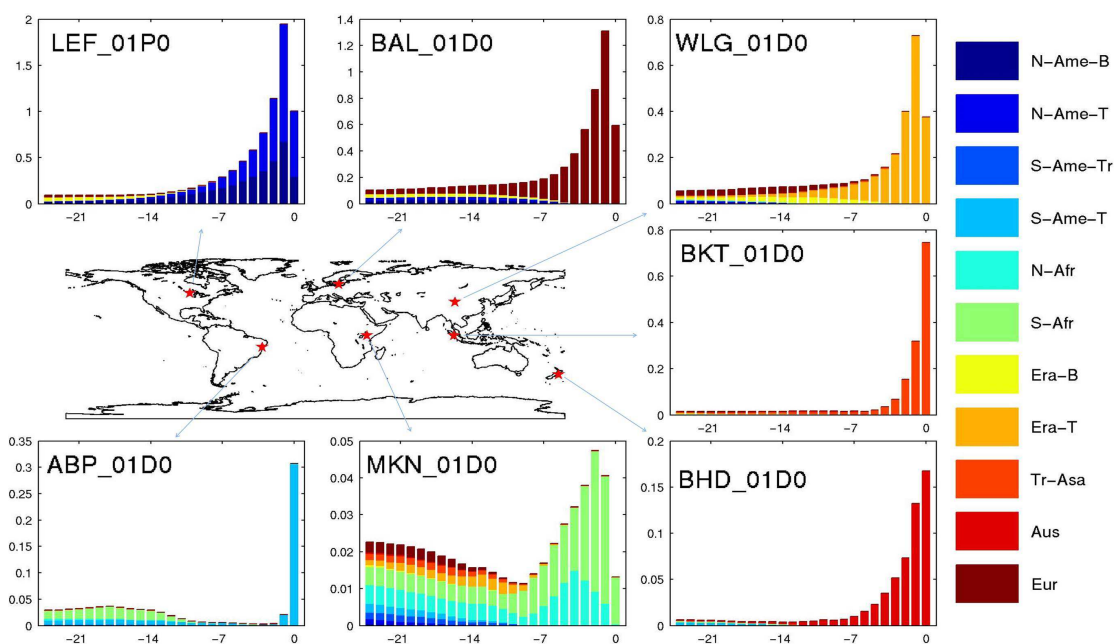
9

1

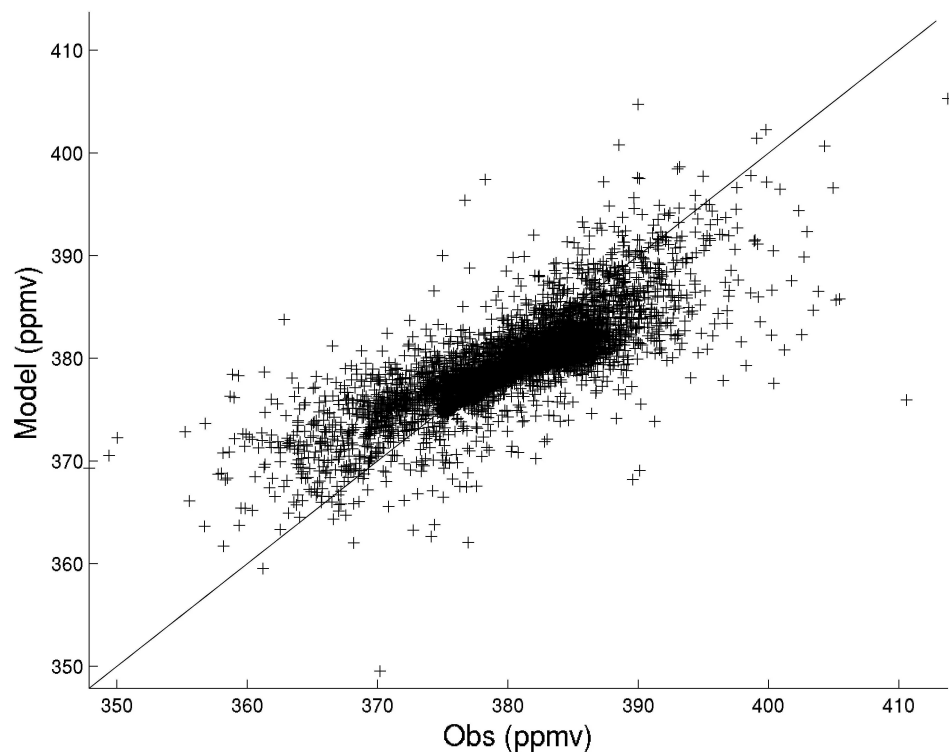
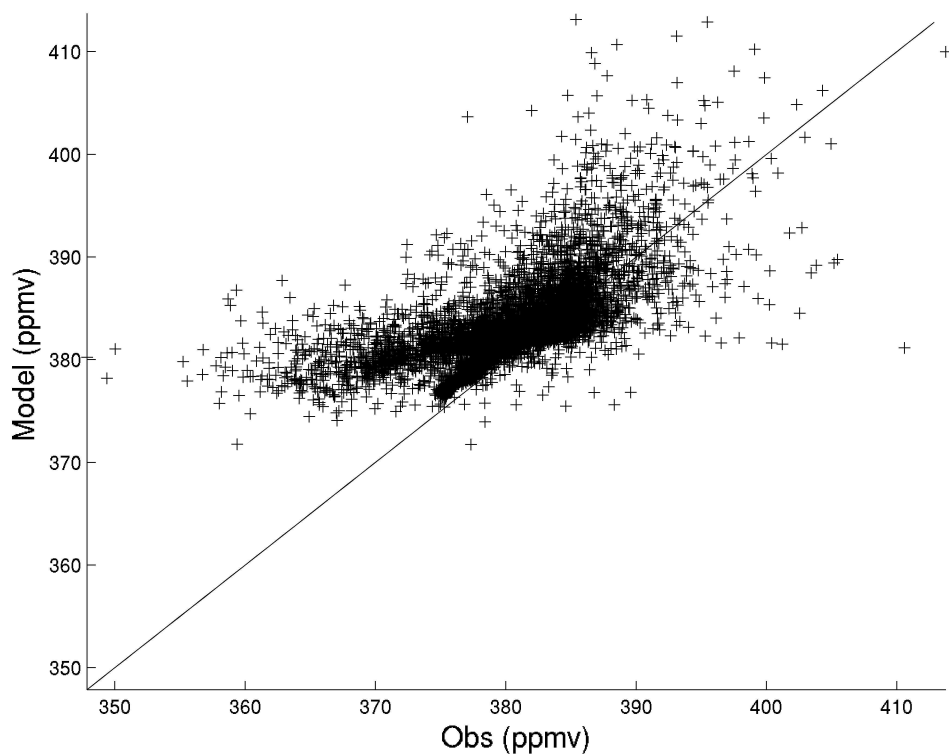


2

3 **Figure 4.** Annual means of carbon budgets (PgC yr^{-1}) on 11 Transcom regions
4 in four different cases. Four cases are associated with prior values modeled
5 with ecosystem model BEPS, assimilated results using GCAS-EK with
6 one-week assimilation windows, two-week windows and three-week windows.
7 11 regions in X-axis refer to 'North American Boreal' (NAB), 'North American
8 Temperate' (NAT), 'South American Tropical' (SATr), 'South American
9 Temperate' (SAT), 'Northern Africa' (NAf), 'Southern Africa' (SAf), 'Eurasia
10 Boreal' (EAB), 'Eurasia Temperate' (EAT), 'Tropical Asia' (TA), 'Australia'
11 (AU) and 'Europe' (EU), respectively
12

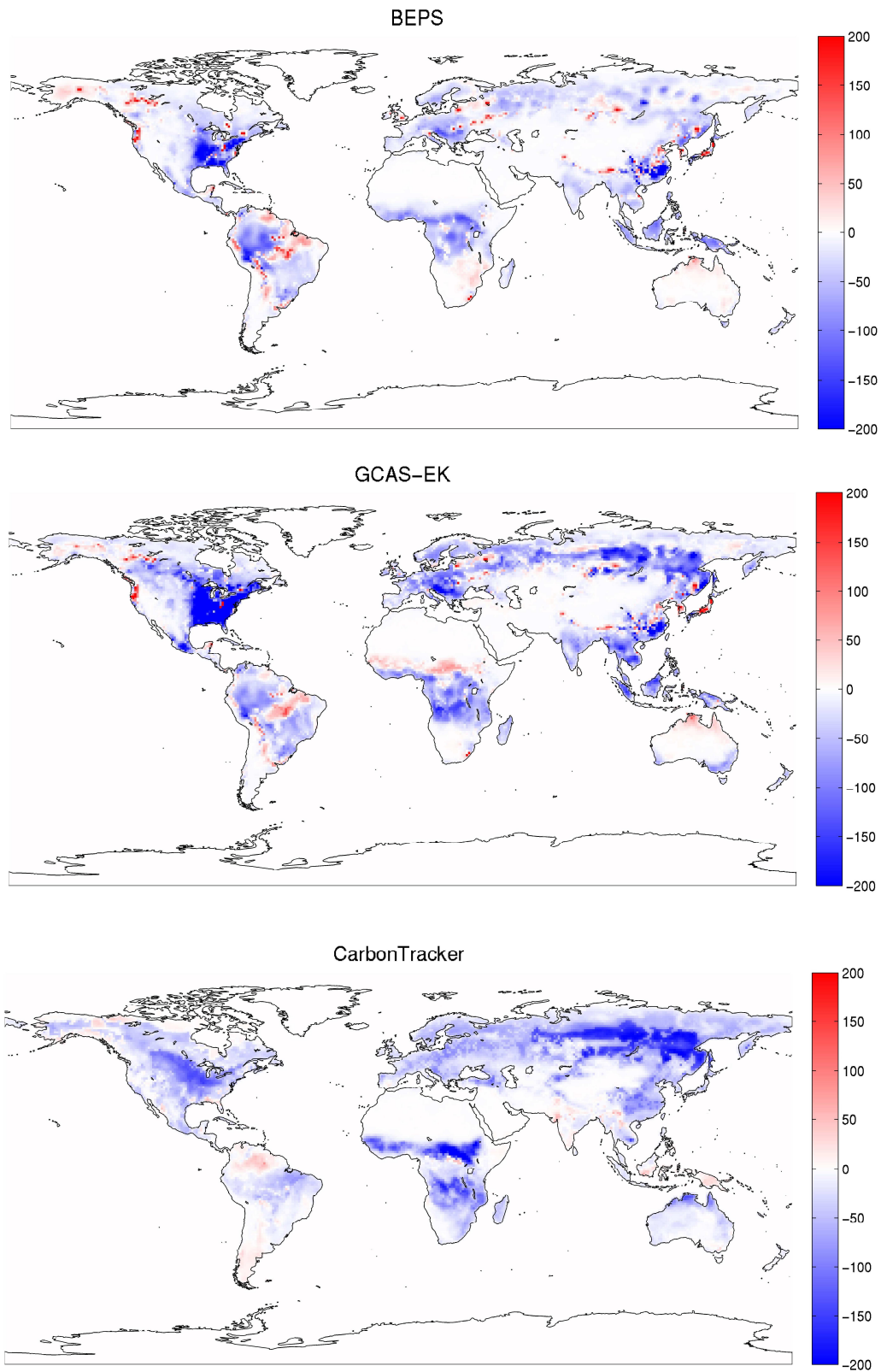


1
 2 **Figure 5.** Mean components of CO₂ concentration at observation sites (Site IDs:
 3 LEF_01P0, BAL_01D0, WLG_01D0, BKT_01D0, BHD_01D0, MKN_01D0
 4 and ABP_01D0) from 11 Transcom regions in each of 25 days before the
 5 observation time. X-axis refers to days before the observation time. Y-axis
 6 refers to the amount of CO₂ concentration in ppm. Different colors within a bar
 7 refer to CO₂ concentration from 11 different Transcom regions. 11 regions
 8 refer to 'North American Boreal' (N-Ame-B), 'North American Temperate'
 9 (N-Ame-T), 'South American Tropical' (S-Ame-Tr), 'South American
 10 Temperate' (S-Ame-T), 'Northern Africa' (N-Afr), 'Southern Africa' (S-Afr),
 11 'Eurasia Boreal' (Era-B), 'Eurasia Temperate' (Era-T), 'Tropical Asia' (Tr-Asa),
 12 'Australia' (Aus) and 'Europe' (Eur) respectively.
 13



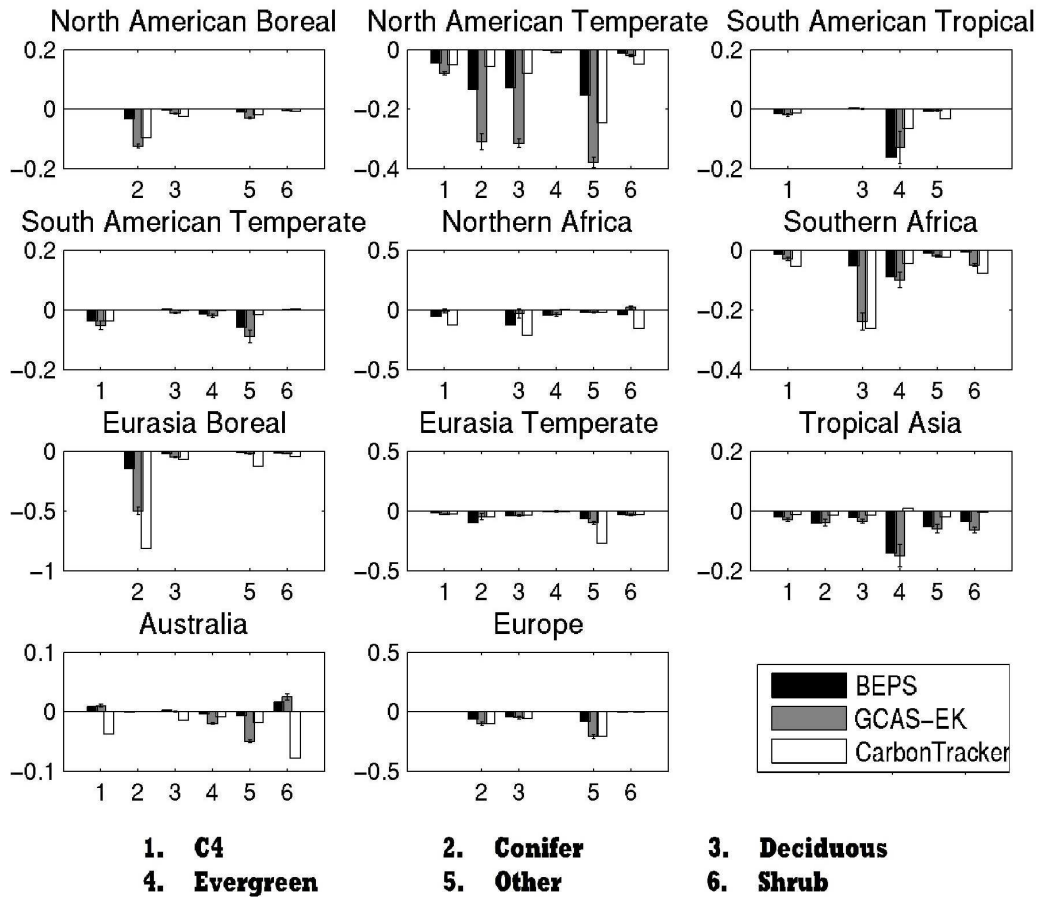
1
 2 **Figure 6.** Comparisons between real observations and simulated concentrations
 3 by control runs: top) control run forcing by prior carbon fluxes; bottom) control
 4 run forcing by assimilated carbon fluxes by GCAS-EK. Both simulations start
 5 from Jan 1,2002 and all simulated concentrations at observation locations and
 6 times in 2005 are compared here.
 7

1

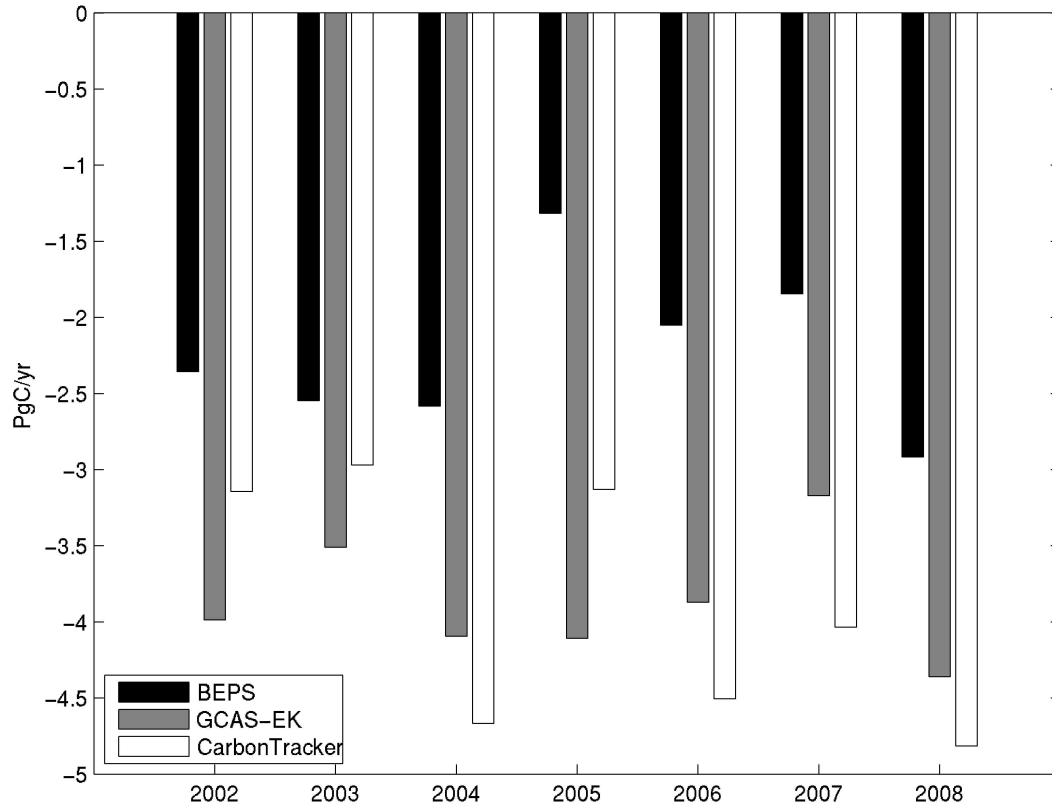


2

3 **Figure 7.** Global carbon budget (gC m⁻²) distributions on multiyear average
4 from 2002 to 2008: prior carbon fluxes simulated by BEPS; assimilated carbon
5 fluxes by GCAS-EK; CarbonTracker 2011 estimated carbon fluxes.



1
 2 **Figure 8.** Annual mean carbon budgets (PgC yr^{-1}) on areas with 6 BEPS plant
 3 function types in Transcom regions from 2002 to 2008. The errors of
 4 GCAS-EK fluxes are the root mean square errors of the ensemble.
 5
 6



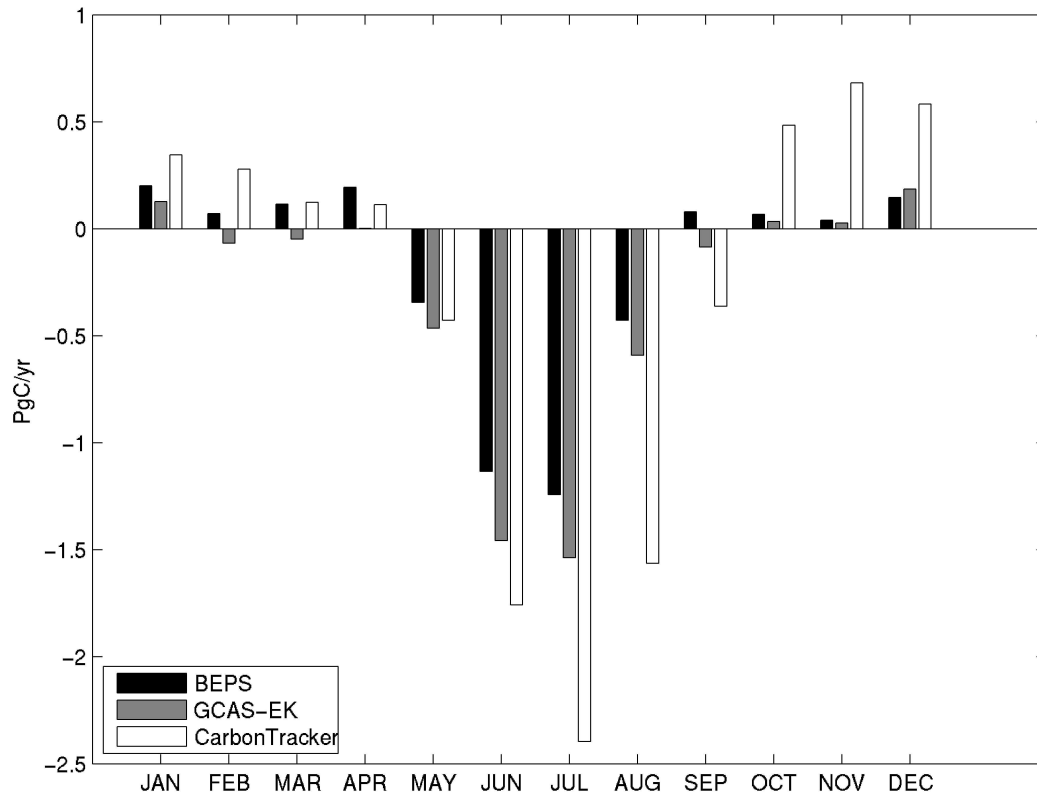
1

2 **Figure 9.** Comparison of interannual variations of global carbon budgets from
 3 2002 to 2008 by three products: BEPS, GCAS-EK and CarbonTracker 2011.

4

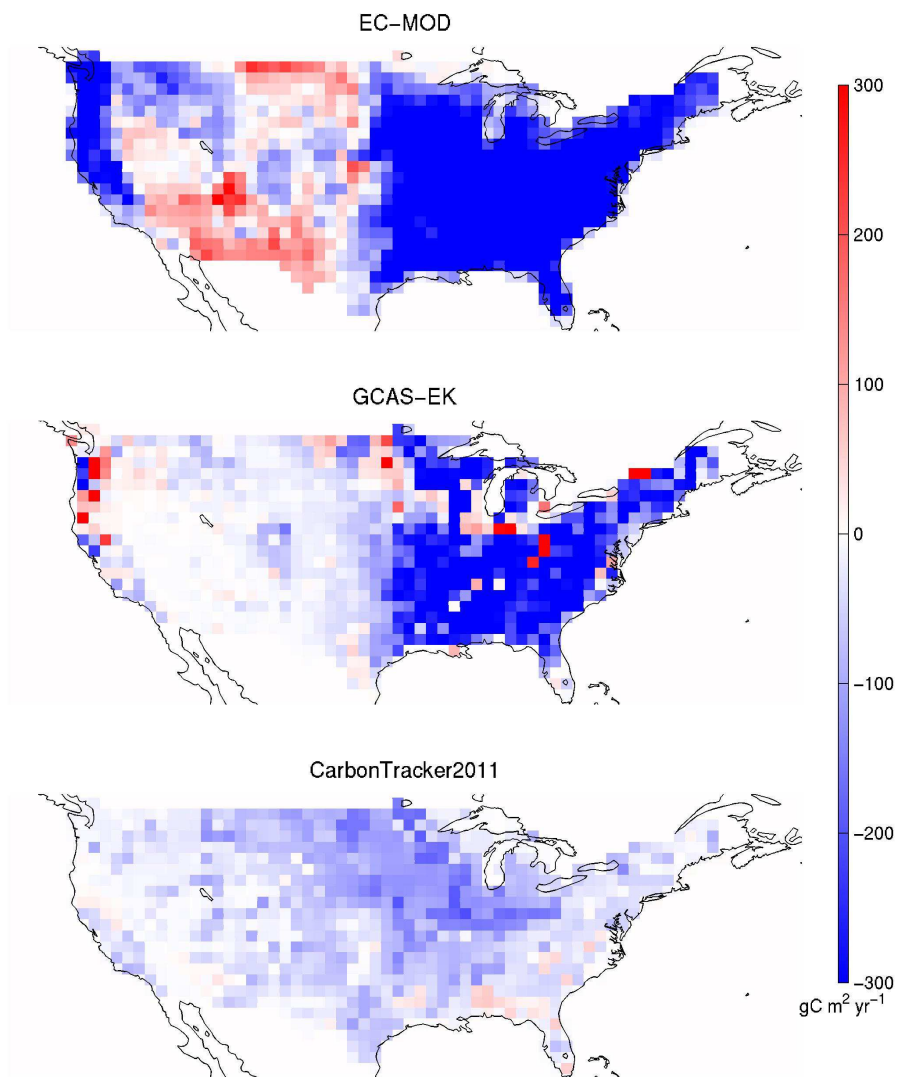
5

6



1
2
3
4

Figure 10. Comparison of multiyear average monthly variations from 2002 to 2008 by three products: BEPS, GCAS-EK and CarbonTracker 2011.



1

2 **Figure 11.** The distribution of averaged net ecosystem exchange ($\text{gC m}^{-2} \text{yr}^{-1}$)
 3 from 2002 to 2006 for conterminous U.S. by EC-MOD, GCAS-EK and
 4 CarbonTracker 2011, respectively. The pattern correlation coefficient is 0.47
 5 between EC-MOD and GCAS-EK, and 0.22 between CarbonTracker 2011 and
 6 EC-MOD.

7